

High-power pump combiners for Tm-doped fibre lasers

D. STACHOWIAK*, P. KACZMAREK, and K.M. ABRAMSKI

Laser and Fibre Electronics Group, Wrocław University of Technology, ul. Wybrzeże Wyspiańskiego 27,
50–370 Wrocław, Poland

In this paper our results of investigation on a pump power combiner in a configuration of 7×1 are presented. The performed combiner, with pump power of 80–85% transmission level, was successfully applied in a thulium doped fibre laser. The performed all-fibre laser setup reached a total CW output power of 6.42 W, achieving the efficiency on a 32.1% level.

Keywords: fibre lasers, thulium-doped fibres, pump power combiners, tapered fibre bundles.

1. Introduction

Thulium-doped fibre lasers (TDFLs), operating in an eye-safe 2 μm spectral range, have found great interest in the last few years due to various possible applications in many fields. For example, such lasers might be used in laser spectroscopy – for detection of trace amounts of molecules and compounds (e.g., greenhouse gases, like carbon dioxide and nitrous oxide) [1], medicine – due to the high water absorption in this spectral range [2–4], optical telecommunication, materials processing, and LIDAR systems [5,6]. Fibre lasers based on Tm-doped active fibres are characterized by a very broad emission bandwidth ranging from 1.7 to 2.1 μm which allows for a tuneable operation in a wide wavelength range [7,8]. A broad absorption band is another important advantage. It gives several alternative capabilities of choosing the pump wavelength [9–13]. One of the popular pumping approaches is to use a fibre laser operating in a 1560–1570 nm range. A pump from this wavelength region was used by M. Jiang *et al.* [14] in a gain-switched TDFL, resulting with a 50% slope efficiency and the peak power of 1 kW. Another approach is to use laser diodes operating at a 790 nm wavelength, where the Tm^{3+} ions have their most prominent absorption peak [15]. The usage of this pumping wavelength allowed to achieve more than 1 kW of output power from a two-stage amplifier, with a 53.2% slope efficiency at a 2045 nm wavelength [16]. Recently also a resonant pumping was proposed for a Tm-doped fibre laser, whereby slope efficiency of 90% is possible to reach. In Ref. 17 slope efficiency of 90.2% of a thulium doped fibre laser with an output power of 1.43 W of 2005 nm was achieved, with a 1.76 W pump power at 1908 nm. Due to the many possible applications and advantages of thulium-doped fibre laser, Tm-doped fibres, as well as the fused components for its all-fibre construction are still being developed [18].

All-fibre design of TDFLs gives many advantages in contrast to lasers based on free-space components. Using passive fibre components instead of bulk optics allows to maintain high beam quality (the beam does not leave the single-mode waveguide). Such construction technique makes the laser setup simple, robust and immune to external factors, like vibrations, contaminations, etc. [6,19]. The most important fibre components in all-fibre lasers are the pump power combiners [20]. The usage of those passive fibre components allows for very efficient coupling of pump power into the active double-cladding fibre on which the high-power lasers are based [21–24]. A typical pump power combiner fabrication is based on tapering of fibre bundle [25]. Usually, power combiners are made in a $N \times 1$ configuration. It means that combiner has N fibres at its input (for the pump power) and one output fibre. The output fibre is typically a passive double-clad fibre. In the case of a fibre amplifier setup, one of the fibres in the bundle is dedicated for signal transmission. This fibre is then surrounded by the pump ports, forming a $(N+1) \times 1$ configuration of the combiner [22]. Usually 105/125 μm multimode fibres with 0.22/0.15 NA are used as input ports for the pump light. As output fibres passive double-clad fibres are used, with the clad diameter from 125 to 400 μm . Commercially available, e.g., from ITF Labs, $N \times 1$ combiners offer a pump power coupling efficiency at the level $> 90\%$ in the case of 125 μm of output fibre clad diameter. For larger diameters of the output fibre offered transmission efficiency the level is $> 93\%$ [26]. In case of pumping methods based on free-space components, end-pumping is the most popular and gives 70–85% coupling efficiency [27,28]. However, application of this method to the laser setup makes the construction very complicated, sensitive for external factors and requires the use of a precise optical and mechanical adjustment. In 2010 Jun Ki Kim and co-workers presented an all-glass pump combiner with the coupling efficiency exceeding 80% [29]. In their approach, the pump combiner consists of multiple pump fibres and an active double-clad

* e-mail: dorota.stachowiak@pwr.edu.pl

fibre spliced to a di-chromatically coated planar convex lens. In Ref. 30 pump power transmission level at 94% in the case of (6+1)×1 combiner was obtained. Performed power combiner was fabricated using tapering process, similar to the process presented in this paper, however, in this particular case the output fibre has a core/clad diameter of 25/250 μm and in our case it is 9/125 μm . There are also reports of fabrication of a pump combiners with a larger number of input ports. In Ref. 31 a 7×1 combiner was first prepared as an inner bundle by fusion tapering process and, then, additional fibres were attached at the outside of the bundle. The whole structure was fused and tapered, creating the final bundle consisting of 14–18 of input ports. The input ports was typically a 105/125 μm multimode fibre and the output fibre was 200/220 μm . The average transmission level reached by this pump combiner was on the 93% level. Pump power combiners are key components in all-fibre systems which allow to keep the setup fully fibreized and immune to external factors. However, commercially available combiners are expensive and are often not customizable, offering only a limited number of input/output fibre types, thus, many researcher groups are still developing topic of pump power combiners and pump combiners with signal feed-through [26,29–37].

2. Fabrication process of a 7×1 pump power combiner

In this paper we demonstrate a high-power Tm-doped fibre laser emitting over 6 W of CW output power, utilizing a home-made pump power combiner. The coupler was performed using a 3SAE LDS system (Large Diameter Splicer) [35], based on a tri-electrode technology. This allows more efficient heating of the fibre because three electrodes are creating so called *Ring Of Fire* – ROF (Fig. 1). Additionally, the system is equipped with an inner cleave blade and allows for profile scanning of fabricated structures.

The system allows to taper down a bundle consisting of several fibres placed in a capillary tube. In our case, seven conventional multimode fibres with core/clad diameter of 105/125 μm and NA = 0.22, were placed in a capillary tube.

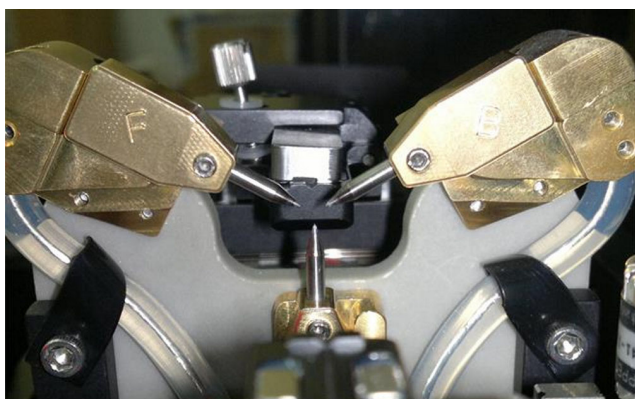


Fig. 1. Three electrodes (ROF) in the LDS System.

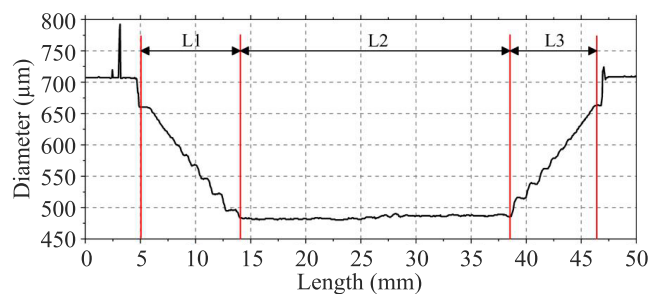


Fig. 2. Profile of tapered capillary tube.

The diameter of a bundle containing seven multimode fibres is 375 μm . Total diameter of a bundle is increased by the thickness of a capillary tube which finally gives a diameter of 500 μm .

In the fabrication process capillary tube with diameters 530/700 μm was used (TSP 530700, Optronis GmbH). The inner diameter is too large for the prepared fibre bundle, thus, the fabrication process includes preparing of a capillary tube. It is tapered down from diameter 530/650 μm to about 400/500 μm . A profile of an exemplary tapered capillary tube is shown in Fig. 2. The most important section of this structure is the section marked as L2. It should be at least 20 mm long, in order to taper it down further in the next steps of the process. In our case the length of the L2 section is about 25 mm. Sections L1 and L3 do not have any influence on parameters of the performed combiner. Main tapering process (tapering of the fibre bundle) covers only L2 section.

Figure 3 shows a cross section area of the prepared capillary tube (approx. a 400 μm inner diameter), and a bundle of seven multimode fibres inserted to this capillary. The filled capillary was afterwards tapered down to the diameter of 150 μm . Recorded profile of the tapered structure is shown in Fig. 4.

The sections L1 and L5 were created during tapering of the capillary tube from 530/650 μm to 400/500 μm (section L1 and L3 from Fig. 2, respectively), and they have not changed. Sections L2, L3 and L4 are a result of tapering process on the capillary tube filled with seven multimode fibres. Total length of the tapered bundle was 18 mm (L2 section). Slight steps in the beginning of section L2 and in

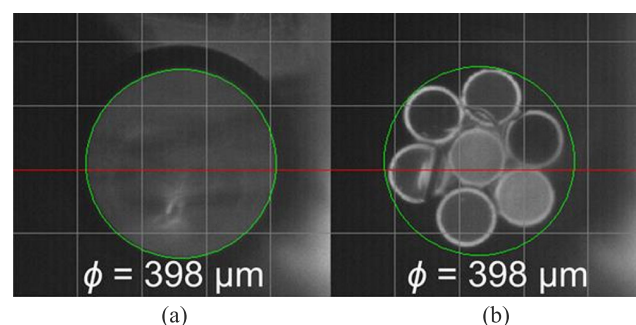


Fig. 3. Cross section area of performed capillary tube (a) and bundle of seven multimode fibre placed inside it.

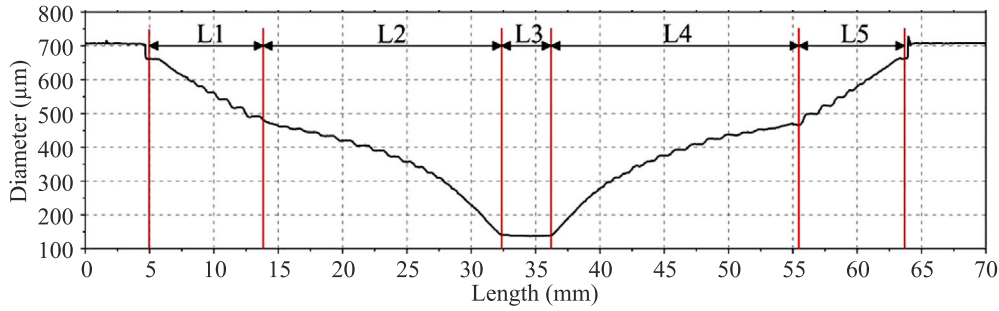


Fig. 4. Profile of tapered fibre bundle.

the end of section L4 can be seen. They are created by specific movements of the ROF. While the fibre bundle is stretched out, the ROF is heating it and scanning many times on proper distance (from left side to the right and *vice versa*). This distance during the whole process is decreasing (from 20 to 3 mm) and this is why we can see a very small L3 section. However, those small steps are a result of changing direction from left to right by the ROF. Because the LDS system provides control on many parameters of the tapering process, those steps can be eliminated by slowing down the stretching speed, which in this case starts from 4 μm/s and accelerates at the end of the process to 40 μm/s. Reducing this speed, as well as the speed of the ROF can help to eliminate those steps.

After tapering process structure was cleaved in Section L3 and spliced to a passive double-clad fibre (Nufern GDF-1550) with a core/clad diameter of 9/125 μm. The cross section area of a cleaved tapered structure is shown in Fig. 5. The external diameter (including capillary tube) is about 150 μm, and the diameter of the fibre bundle inside the capillary is about 110 μm. Similar fabrication process was presented in Ref. 36, where a power combiner in a (N+1)×1 configuration was shown.

Fabricated structure was closed in an aluminium housing in order to provide proper heat dissipation. The trans-

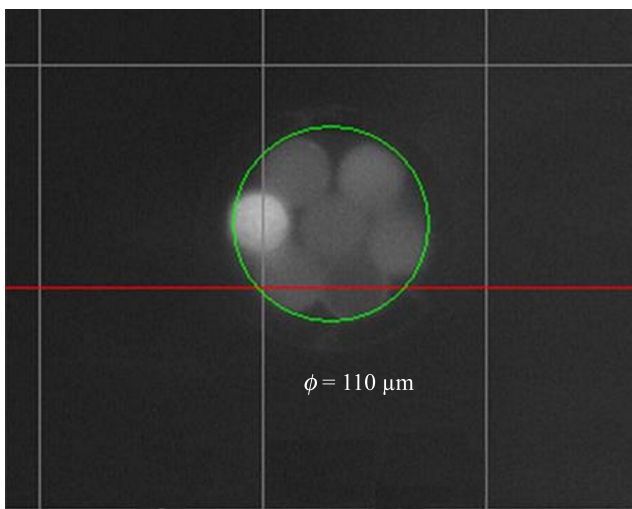


Fig. 5. Cross section area of cleaved fibre bundle after tapering process.

mission for each multimode port varies from 80% up to 85%. The highest transmission level was achieved for the centrally located fibre, thanks to its best coupling with the clad of the output passive fibre. In Ref. 36 efficiency of a fabricated (6+1)×1 power combiner based on a single-mode feed-through signal fibre and a 9/125 μm double-clad output fibre was on the level of 68–72%, so we can see that some improvements in the fabrication process was made. However, in the same work the combiner in a configuration of (6+1)×1, but based on the LMA feed-through fibre (20/125 μm) and an output fibre of 25/300 μm, was also presented. In the case of a pump and signal combiner based on LMA fibres transmission of pump power was achieved on much higher level: 96–99%, so the efficiency of the (7×1) pump power combiner fabricated in this work is much below these results. On the other hand, this is the first result in the case of this pump combiner configuration and even though it requires an optimization of the tapering process, the result is better than in the case of (6+1)×1 pump and signal combiner with the same output double-clad fibre presented in Ref. 36. It was easier to achieve high transmission level in the case of a pump and signal power combiner presented in our previous work (with LMA output 25/300 μm fibre). This is because the outer diameter of the output fibre was very large – 300 μm, so the fibre bundle consisting of 6 multimode fibres (105/125 μm) and one signal LMA fibre (20/125 μm) was tapered down with a very small taper ratio (TR = 1.3). In the case of the 7×1 pump combiner presented in this work the taper ratio is much larger (TR = 3), and it has a great influence on the fabricated power combiner transmission level. Minor losses can be caused by small steps in the shape of the taper. Higher distortion of the profile was observed in Ref. 36 where very high transmission efficiency was observed. Pump combiner losses can be easily estimated by the brightness ratio, which is defined as [37]

$$BR = \frac{D_{out}^2 NA_{out}^2}{n D_{in}^2 NA_{in}^2},$$

where D_{out} and D_{in} are the diameters of output and input fibres, NA_{out} and NA_{in} are the numerical apertures of those fibres and n is the number of input ports. It is suggested that the BR for the designed combiner should have a value equal or higher than 1 to achieve a power combiner with no losses. In the case of the combiner (based on LMA fibres) pre-

sented in Ref. 36 the BR parameter is > 5 , thus, we have a high transmission level (97–99%). In this case the BR is > 0.88 , therefore, some losses resulting from tapering to the outer diameter of an output fibre are unavoidable. Additionally, losses are enlarged by cleaving and splicing, but these processes are easy to optimize because of a smaller outer diameter than in the case of the combiner from Ref. 36. Some losses can be also caused by a non-linear shape of the taper. Defects such as shape of the profile, slight steps on it, cleaving and splicing have some influence on the pump signal attenuation, but they can be optimized. Another thing that affects the transmission is tension of the bundle during the tapering process. It should remain on the 0–5 g level during the whole process. In this specific case the tension raised in the last part of the tapering process resulting in stresses inside the bundle. This drawback can be offset by increasing the power of the ROF in the last part of the process.

The fabricated coupler was tested in the case of backward propagated radiation. This phenomenon can spontaneously occur in a laser or amplifier configuration and cause damage of the pumping laser. In this experiment, a 25 mW signal at 1550 nm wavelength was launched to the DC output of the combiner. At ports from 2 to 7 (which surround central port no. 1) this signal was successfully suppressed by 23 dB. However, almost 90% of the launched 1550 nm signal is transferred to the central port (which is placed in the middle of the bundle). This centrally placed fibre, beside good coupling with the clad, has good coupling with the core of the output fibre. This is the reason of the smallest attenuation of backward propagated radiation which poses a high risk of a possible damage of the pump source launched to this port. Therefore, the central port should not be used for pumping, however, other six multimode ports can be safely used.

Long term behaviour of the fabricated combiner was verified using four 915 nm multimode laser diodes spliced to 4 ports of the combiner (total power of 36 W) and launched for a period of 1 hour. The temperature of the combiner did not exceed 55°C and the transmission of each port maintained unchanged.

3. Application of fabricated pump power combiner in a thulium-doped fibre laser

The fabricated combiner was applied in a high-power Tm-doped fibre laser in a linear cavity configuration. Our experimental setup is shown in Fig. 6.

The laser setup was based on a 3 m long Tm-doped active fibre (CoreActive – DCF-TM-10/128). It was forward pumped by five ~790 nm laser diodes (LUMICS–LU0793T040-QD05N12A) with a maximum total pump power of 20 W (each diode emits 4 W). Fibre Bragg gratings (FBGs) on double-clad fibres were used as both mirrors in the resonator. The FBG at the input has a FWHM bandwidth of 1.06 nm, a peak reflectivity higher than 99% at

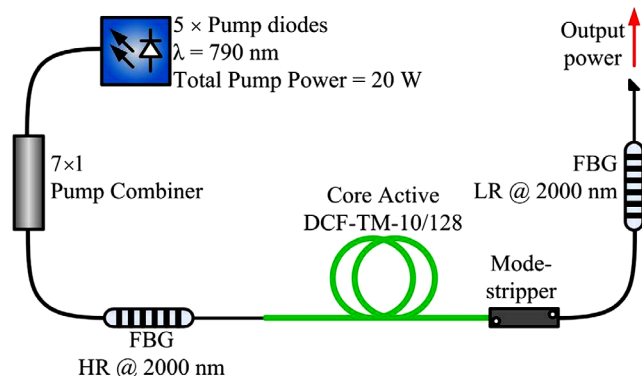


Fig. 6. Scheme of the experimental setup.

2000 nm, and over 94% transmission for the 793 nm pump wavelength. The output FBG has 0.5 ± 0.2 nm bandwidth, and peak reflectance at the level of $10 \pm 2\%$ for 2000 nm. Both FBGs were made on double-cladding fibres with a 10 μm core diameter, matched to the active fibre. This allows to avoid splicing losses caused by core diameter mismatch.

For pumping an active double clad fibre, a fabricated power combiner was used. There was available five laser diodes, thus only five from seven input ports of the combiner were used. Because of a very low attenuation of backward radiation of the central port, it will not be used in the laser setup for the safety reason. Pumping radiation of 20 W was launched through five combiner ports (from port no. 2 to port no. 6). A graph showing the output power vs. the pump power is presented in Fig. 7.

The maximum achieved output power was 6.42 W at 20 W of pumping power. The slope of efficiency was at the level of 32.1% and no decrease in the slope was observed. The manufacturer of the used active fibre in our setup reports the slope efficiency of 47% [38]. The cause of a lower efficiency of our experimental setup is that it was not optimized yet. Each splice between fibre components may result in some attenuation, nevertheless, the highest attenuation

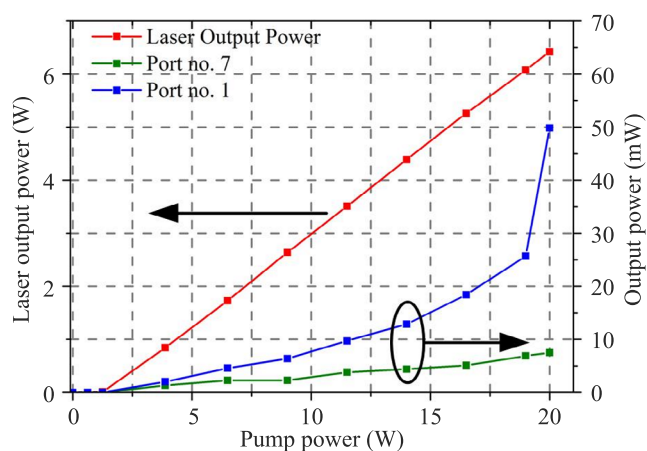


Fig. 7. Laser output power vs. pump power and the result of measurement of the backward radiation through free ports of the combiner.

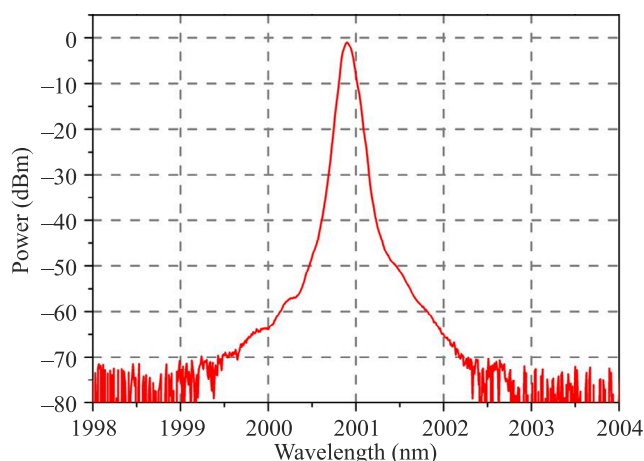


Fig. 8. Optical spectrum of the 2000.9 nm output signal.

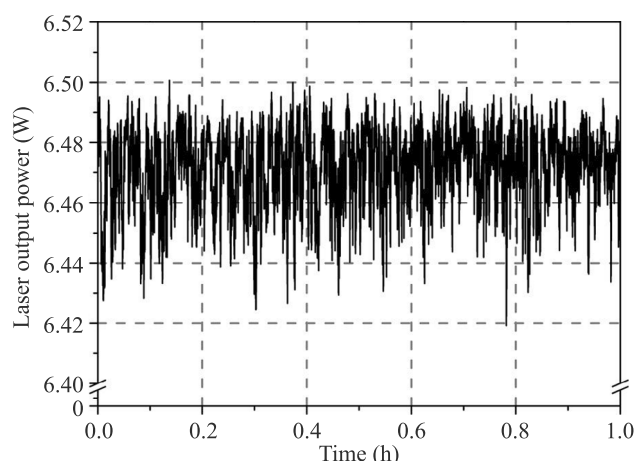


Fig. 9. Laser output power stability.

and reason of a low slope of efficiency is performed pump power combiner which has a pump power coupling efficiency on a 80% level. It means that only 16 W (from 20 W) is launching into the active double clad fibre. Our laser setup itself clearly requires optimization, but the major losses are caused by the combiner.

In Fig. 7 it can be also seen that in the case of port no. 1 the backward radiation is rapidly increasing with the highest launched pump power. The maximum power recorded on port no. 1 reached about 50 mW in comparison to less than 10 mW on port no. 7. This shows that despite the higher transmission of the central fibre, it should not be used as a pumping port. This fibre should be cleaved at some angle to avoid possible refraction of its end face or used as a tap monitor.

The recorded optical spectrum for maximum pump power is shown in Fig. 8. The output signal is characterized by the optical signal to noise ratio (OSNR) at the level of almost 70 dB, and FWHM of 0.13 nm.

Figure 9 shows the measured output power stability over 1 hour period. It can be seen that the fluctuations are very small and the calculated output power variation is at the level of 1.23%.

4. Conclusions

In conclusion we have demonstrated a Thulium-doped fibre laser with a self-fabricated pump power combiner with 7 multimode pumping ports and a 9/125 μm double-clad fibre at its output. The pump coupling efficiency for seven multimode input fibres reaches 80–85% which is very satisfactory. Taking into account the cost efficiency of self-fabricated combiner, and the results achieved so far, an all-fibre pumping scheme seems to be an excellent alternative to the free-space coupling. We believe, that further optimization of the fabrication process will allow to achieve higher transmission, reaching 90–95%. Such improvement could be achieved by changing tapering parameters or improving cleaving and splicing process. The fabricated combiner was

successfully applied in a Thulium-doped fibre laser setup, capable of generating 6.42 W of CW power at 2000.9 nm wavelength, in the presence of 20 W of pumping power.

Acknowledgements

The work presented in this paper was supported by Wrocław Research Centre EIT+ under the project “The Application of Nanotechnology in Advanced Materials” – NanoMat (POIG.01.01.02-02-002/08) financed by the European Regional Development Fund (Innovative Economy Operational Programme, 1.1.2)

References

1. F.K. Tittel, D. Richter, and A. Fried, “Mid-infrared laser applications in spectroscopy”, *Solid-State Mid-Infrared Laser Sources* **89**, Topics in Applied Physics, Springer Berlin Heidelberg, 445–516 (2003).
2. N. M. Fried and K. E. Murray, “High-power thulium fibre laser ablation of urinary tissues at 1.94 μm ”, *J. Endourol.* **19**, 25–31 (2005).
3. N.M. Fried, “High-power laser vaporization of the canine prostate using a 110 W thulium fibre laser at 1.91 μm ”, *Lasers Surg. Med.* **36**, 52–56 (2005).
4. K.D. Polder and S. Bruce, “Treatment of melisma using a novel 1,927-nm fractional thulium fibre laser: a pilot study”, *Dermatol. Surg.* **38**, 199–206 (2012).
5. W. Wu, T. Yu, Q. Huang, X. Cheng, and W. Chen, “16W Average Power 2 μm Thulium fibre laser with one stage MOPA”, *Proc. of SPIE* **9080**, 908008–7 (2014).
6. W. Shi, Q. Fang, X. Zhu, R.A. Norwood, and N. Peyghambarian, “Fibre lasers and their applications [Invited]”, *Appl. Opt.* **53**, 6554–6568 (2014).
7. D.Y. Shen, J.K. Sahu, and W.A. Clarkson, “High-power widely tunable Tm:fibre lasers pumped by an Er,Yb co-doped fibre laser at 1.6 μm ”, *Opt. Express* **14**, 6084–6090 (2006).
8. D.C. Hanna, R. Percival, R.G. Smart, and A.C. Tropper, “Efficient and tuneable operation of a Tm-doped fibre laser”, *Opt. Commun.* **75**, 283–286 (1990).

9. Y. Sintov, M. Katz, P. Blau, Y. Glick, E. Lebiush, and Y. Nafcha, "A frequency doubled gain switched Yb³⁺-doped fibre laser", *Proc. SPIE* **7195**, 719529–8 (2009).
10. J. Geng, Q. Wang, T. Luo, B. Case, S. Jiang, F. Amzajerjian, and J. Yu, "Single-frequency gain-switched Ho-doped fibre laser", *Opt. Lett.* **37**, 3795–3797 (2012).
11. Y. Tang and J. Xu, "Hybrid-pumped gain-switched narrow-band thulium fibre laser", *Appl. Phys. Express* **5**, 072702–3 (2012).
12. Y. Tang and J. Xu, "High power tuneable Tm³⁺-fibre lasers and its application in pumping Cr²⁺:ZnSe lasers", *Frontiers in Guided Wave Optics and Optoelectronics*, Vol. **20**, pp. 403–471, Bishnu Pal (Ed.), ISBN: 978-953-7619-82-4, InTech, 2010.
13. Y. Tang and J. Xu, "High-power pulsed 2-μm Tm³⁺-doped fibre laser", *Semiconductor Laser Diode Technology and Applications*, Dr. Dnyaneshwar Shaligram Patil (Ed.), Vol. **16**, pp. 287–321, ISBN: 978-953-51-0549-7, InTech, 2012.
14. M. Jiang and P. Tayebati, "Stable 10 ns, kilowatt peak-power pulse generation from a gain-switched Tm-doped fibre laser", *Opt. Lett.* **32**, 1797–1799 (2007).
15. S.D. Jackson and T.A. King, "Theoretical modelling of Tm-Doped silica fibre lasers", *J. Lightwave Tech.* **17**, 948–956 (1999).
16. T. Ehrenreich, R. Leveille, I. Majid, K. Tankala, G. Rines, and P.F. Moulton, "1kW, all-glass Tm:fibre laser", *Proc. SPIE* **7580**, 112 (2010).
17. D. Creedon, B.R. Johnson, S.D. Setzler, and E.P. Chicklis, "Resonantly pumped Tm-doped fibre laser with > 90% slope efficiency", *Opt. Lett.* **39**, 470–473 (2014).
18. P. Peterka, P. Honzátko, I. Kašík, J. Cajzl, and O. Podrazký, "Thulium-doped optical fibres and components for fibre lasers in 2 μm spectral range", *Proc. SPIE* **9441**, 94410B-6 (2014).
19. D.J. Richardson, J. Nilsson, and W.A. Clarkson, "High power fibre lasers: current status and future perspectives", *J. Opt. Soc. Am. B* **27**, B63–B87 (2010).
20. D. Noordegraaf, M.D. Maacka, P.M.W. Skovgaard, J. Johansena, F. Beckerb, S. Belkeb, M. Blomqvistc, and J. Lægsgaardd, "All-fibre 7×1 signal combiner for incoherent laser beam combining", *Proc. of SPIE* **7914**, 79142L-1 (2011).
21. F. Gonthier, L. Martineau, N. Azami, M. Faucher, F. Seguin, D. Stryckman, and A. Villeneuve, "Highpower all-fibre components: the missing link for high-power fibre lasers", *Proc. SPIE* **5335**, 266–276 (2004).
22. A. Braglia, A. Califano, Y. Liu, and G. Perrone, "Architectures and components for high power CW fibre lasers", *Int. J. Modern Phys. B* **28**, 1442001-14 (2014).
23. G. Sobon, P. Kaczmarek, D. Sliwinska, J. Sotor, and K. Abramski, "High-power fibre-based femtosecond CPA system at 1560 nm", *IEEE J. Selected Topics in Quantum Electron.* **20**, 492–496 (2014).
24. G. Sobon, D. Sliwinska, K.M. Abramski, and P. Kaczmarek, "10 W single-mode Er/Yb co-doped all-fibre amplifier with suppressed Yb-ASE", *Laser Phys. Lett.* **11**, 025103 (2014).
25. B. Wang and E. Mies, "Review of fabrication techniques for fused fibre components for fibre lasers", *Proc. of SPIE* **7195**, 71950A-11(2009).
26. [http://www.itflabs.com/data/File/Tech/Data_Sheets_2012/E%20\(HPPC%20DCF\).pdf](http://www.itflabs.com/data/File/Tech/Data_Sheets_2012/E%20(HPPC%20DCF).pdf)
27. J. Swiderski, A. Zając and M. Skorczakowski, "Pulsed ytterbium-doped large mode area double-clad fibre amplifier in MOFPA configuration", *Opto-Electron. Rev.* **15**, 98–101 (2007).
28. Y. Jeong, S. Yoo, Ch.A. Codemard, J. Nilsson, J.K. Sahu, D.N. Payne, R. Horley, P.W. Turner, L. Hickey, A. Harker, M. Lovelady, and A. Piper, "Erbium:Ytterbium codoped large-core fibre laser with 297-W continuous-wave output power", *IEEE J. Selected Topics In Quant. Electron.* **13**, 573–579 (2007).
29. J.K. Kim, Ch. Hagemann, T. Schreiber, T. Peschel, S. Böhme, R. Eberhardt, and A. Tünnermann, "Monolithic all-glass pump combiner scheme for high-power fibre laser system", *Opt. Express* **18**, 13194–13203 (2010).
30. A. Braglia, M. Olivero, A. Neri, G. Perrone, "Fabrication of pump combiners for high power fibre lasers", *Proc. of SPIE* **7914**, 79142V-1 (2011).
31. B.H. Kima, S.J. Kimb, Y. Yoonb, and S. Hannc, "Fabrication of the reliable (14–18)×1 fibre laser power combiner by the novel double bundling method", *Proc. of SPIE* **8621**, 862118-3 (2013).
32. D.L. Sipes, J.D. Tafoya, D.S. Schulz, B.G. Ward, and C.G. Carlson, "Advanced components for multi-kW fibre amplifiers", *Proc. of SPIE* **8237**, 82370P-1 (2012).
33. D. Neugroschl, J. Park, M. Wlodawski, J. Singer, and V.I. Kopp, "High-efficiency (6+1)×1 combiner for high power fibre lasers and amplifiers", *Proc. of SPIE* **8601**, 860139-1 (2013).
34. P. Koška, Y. Baravets, P. Peterka, J. Bohata, and M. Pisarik, "Mode-field adapter for tapered-fibre-bundle signal and pump combiners", *Appl. Opt.* **54**, 751–756 (2015).
35. R. Wiley and B. Clark, "High-power, fused assemblies enabled by advances in fibre-processing technologies", *Proc. SPIE* **7914**, 79140F (2011).
36. D. Sliwinska, P. Kaczmarek, and K.M. Abramski, "Tapered fibre bundle couplers for high-power fibre amplifiers", *Proc. of SPIE* **9441**, 94410G-1 (2014).
37. B. Sévigny, P. Poirier, and M. Faucher, "Pump combiner loss as a function of input numerical aperture power distribution", *Proc. SPIE* **7195**, 719523 (2009).
38. http://www.coractive.com/pdf/datasheets/DCF-TM-10_128_DS100619r02.pdf